Available online at www.jcsonline.in Journal of
Current Science & Humanities
12 (2), 2024, 30-42

Circular modeling of birdsong production as a function of temperature

Mr.V.Karunakar, Mr.Krishnakanth, Mrs.B.Vidhya
ASSIT.PROFESSOR[1,3], ASSOCIATE PROFESSOR[2]
H&S(Physics)
SWARNA BHARATHI INSTITUTE OF SCIENCE & TECHNOLOGY (SBIT)

Abstract

Much discussion has centered on the question of what exactly the brain processes in the birdsong motor pathway are that cause the production of respiratory rhythms. The telencephalic nucleus HVC governs a distinct temporal domain in a top-down control paradigm, from which additional brain areas are engaged downstream to produce vocal gestures. The idea that the neural network generates motor instructions in a dispersed fashion, with instructions flowing upstream and downstream, is another plausible explanation. The incorporation of many timescales yields the musical composition in this circular design. We used local focal cooling of HVC in canaries to alter the timeline existing there and therefore clarify these perspectives. We fit the experimental pressure patterns of various sorts of syllables—which compose an entire song—within the circular model. We prove that in order to recreate them, at least two distinct timelines, one of which is cooled and the other left untouched, are required. This frame statistically recreated the syllable alterations, including stretching and breaking.

Introduction

Birdsong is a remarkable example of how a complex behavior emerges from the interaction of peripheral motor areas and the central nervous system. The song motor pathway, which comprises the regions in the bird's brain that generate motor instructions for singing, involves several nuclei. These are located in the telencephalon, thalamus and brainstem [1–5]. The integration of the activity within them gives rise to vocal motor sequences.

To generate a song, the brain motor pathway commands the activities of the respiratory system and the vocal organ called syrinx, a bipartite structure located between the bronchi and the trachea. The result is a succession of pressure gestures that are in a delicate coordination with the muscle activity in the syrinx [6–9]. These are commonly designated as syllables, which are the smallest units of a song, usually separated by silent gaps when the bird inspirates. The wall membranes in the syrinx —labia— generate sound by modulating the airflow coming from the air sacs. Therefore, since the generation of sound requires establishing airflow across the syrinx, a central aspect of motor control is its capacity to generate diverse respiratory rhythms [10]. We show in Fig. 1(A) an example of pressure in the air sacs during a song in domestic canaries (*Serinus canaria*), where different patterns can be distinguished. The song starts with a long expiratory pulse that consists of a series of small pressure

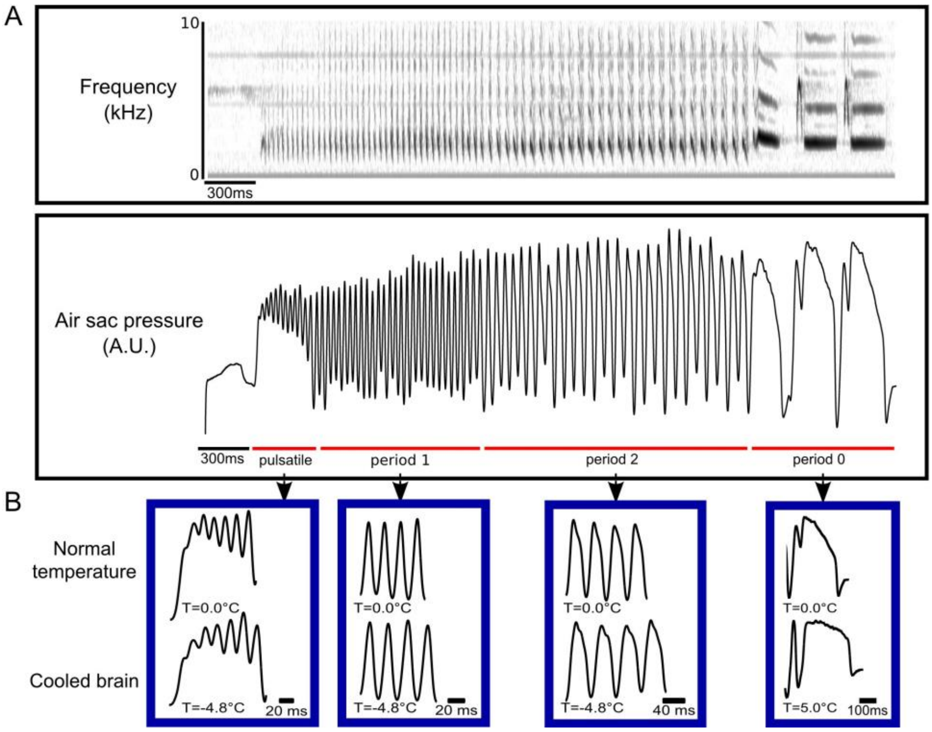

Figure 1: **Respiratory patterns of canary songs at different HVC temperatures.** Experimental measurements of pressure in the air sacs during the canary song. (A) Top: Sonogram of a complete song. Bottom: Different breathing patterns can be identified depending on their morphology and duration: Pulsatile gestures characterized by respiratory fluctuations mounted on a constant value, period 1 and period 2, displaying oscillating patterns and period 0 (repeated three times), ending with long expiratory pulse. (B) When cooling the nucleus HVC with a Peltier cooling device, a stretching in all the syllables is observed. In particular, the p0 syllables also show a change in their morphology.

pulses mounted on a DC level, each of them knownas “pulsatile” pattern. It is followed by a repeating gesture of larger amplitude, with an oscillation reminiscent of harmonic pulses. These are designated as period 1 gestures (p1). Right after, we can seea p2 pattern, which also displays oscillations, but of approximately twice the duration of p1 syllables. Finally, the last syllables in the example (p0) are repeated with the lowest frequency and present a brief expiratory pulse followed by a decaying expiration. It has been shown that the vast majority of syllables can be classified into these four groups according to its frequency [11]. Fastest syllabic rates (> 27 Hz) correspond to pulsatile syllables, while syllabic repetition rates between 13 and 25 Hz correspond to p1 pressure patterns. Lower syllabic rates, ranging between 8 and 12 Hz are identified as p2 patterns whereas rates in the range of_2 5 Hz fall in the classification of p0 patterns. Within these groups, different types of syllables can be classified according to its morphological difference such as number of pressure peaks and average time of expiration.

How these respiratory patterns emerge from the neural activity along the song motor pathway is still an open question. One hypothesis was presented as a top-down model [12–14]. In this framework, the telencephalic nucleus HVC (used as a proper name) which is synaptically far from the vocal organ (at least two synapses until reaching the brainstem), is placed as the highest element of the hierarchy. a sequence of bursts of about 10 ms duration, this area is conjectured to drive the activation of the neurons in the RA (nucleus robustus of the archis-triatum). RA neurons recruit in turn the brainstem motor neurons downstream. The complexity of the vocal gestures, therefore, emerges from a cascade of information ruled by a unique temporal sequence (HVC clock time) in this top-down hierarchy rep- resentation, diminishing the role of the bottom-up feedback arriving to HVC from the brainstem.

In an alternative hypothesis, the activation of the neuronal nuclei responsible for respiration may not only be due to the activity in the telencephalic area flowing downstream but also to the activation in other regions within the brainstem [15–18]. This does not mean that the timing signals in HVC do not play a crucial role, but that the system has to be analyzed in an integral fashion. A computa- tional model was developed to represent this pro- posed architecture in the work of Alonso *et al.* [15]. In this framework, neural populations in the brain-stem are connected upstream via the thalamus with HVC, which provides an architecture that gives the model its name: circular model. The generation of pressure patterns is therefore obtained by integrat- ing the activity of two separated, yet connected, inputs: one from HVC and the other within the brainstem. This structure suggests the existence of more than one timescale involved, as the infor- mation coming from the brainstem is processed by HVC and then flows back into the brainstem where it combines with the original signal.

Thermal manipulation of nuclei of the motor pathway is a way that researchers in the field use to report evidence that could only be explained in one of the two presented paradigms. By locally cooling both left and right HVC nuclei in zebra finches, ca- naries and Bengalese finches, it was observed a sig-nificant temporal stretching across all time scales, from song motif to silent gaps [14, 19–23]. From re- cent works exploring temperature effects at a neu- ronal level [24], we know that synaptic conduc-tance propagation times coming from HVC's affer-ents are slowed with temperature, being then plau-sible to expect an expansion in the motor gesture. The stretching is then consistent with the top-down model. However, more recently, Hamaguchi *et al.* explored cooling the afferent nucleus to HVC in the thalamus, Uva thalamic nucleus uvaeformis, and showed that the reported values of stretching re- quire an integrated architecture [22]. In addition, it was shown by Goldin *et al.* [19] that cooling HVC nuclei below 5°C results in the "breaking" of the syllables in the song of canaries into shorter motifs and in the appearance of complex respiratory pat- terns. In that work, the authors showed that some breaking patterns can be qualitatively explained by modeling the activity in HVC and in an unallocated brain area downstream, with a simple dynamical system driven near a bifurcation region. Although explaining some of the breaking patters within the model, not all syllable changes could be accounted for. One example of such elusive modification is shown in Fig. 1(B) (p0 "breaking"). The alter- ation of the timescale of a part of the entire p0 syllable as HVC is cooled pointed out the need of considering other brain areas or the exploration of different architectures for advancing the building of a model for song production.

In this work, we use the circular model to ex-plain the different types of syllable "breakings", which conjectures that this phenomenon can be ex- plained as a product of the interaction between two timescales. This model not only includes the one discussed in Goldin *et al.*, but it also allows to ex- plain the structural changes of the p0 syllables. By quantitatively fitting experimental data of singing canaries at different HVC cooling temperatures, we unveil a mechanism of pulsatile, p1 and p2 stretch-ing, as well as p0 stretching and breaking. For the last type of syllables, we show that the breaking is a natural consequence of the slowing of the activity in the telencephalon during thermal manipulation of HVC while keeping the brainstem activity unchanged. As each syllable type needs a different pattern of activity in our model, we support a recent view in which different parallel pathways are represented anatomically in HVC [25, 26].

Materials and methods

Experiments

All experiments were approved by the Institutional Animal Care and Use Committee of University of Buenos Aires (FCEN-UBA). We recorded the air sac pressure activity using a flexible cannula which was inserted through the abdominal wall into the anterior thoracic air sac under isoflurane anesthesia. A miniature piezoresistive pressure transducer
(Fujikura model FPM-02PG) mounted on the canary's back was connected to the cannula [6]. The voltage output from the transducer was amplified and recorded with a data acquisition device (National Instruments BNC2110). In addition, a cooling device that consisted in a Peltier cell was used to cool both left and right HVC nuclei [19].

Measurements consisted of recordings of song and pressure without cooling in the first place. Then, we proceeded to thermally manipulate the telencephalic nucleus by lowering the temperature by 1°C every two minutes, until the desired temperature was reached. After two minutes at the respective temperature, recording was started. Once sufficient data were collected, we continued with further cooling.

This procedure was repeated for at least four cooling temperatures in the range of 0°C to 7.4°C in three male adult canaries. A database of over 36 minutes of songs and pressure patterns was obtained. We extracted for the analysis 222 pulsatile syllables, 552 p0, 203 p1 and 1366 p2.

The computational model

We present a mathematical description of the circular model which was previously introduced in Ref. [15]. The authors proposed an average description of the activity of each intervening area of the motor pathway, modeling it with a neural additive model. The equations governing the dynamics are phenomenological and connections between areas reflect a circular architecture [see Fig. 2(A)]. In what follows, we will describe in detail the variables, the connectivity and how the activity starting in the brainstem goes upstream, then downstream and integrates back with the initiating signal that traveled through another path within the brainstem.

Motor activity is identified with the dynamics of an expiratory related area ER [putatively the nucleus retroambigualis (RAm), black circle, Fig. 2(A)]. This region is part of the respiratory circuit within the brainstem and it is composed of two populations of interconnected neurons, one excitatory and another inhibitory (ER_e and ER_i, respectively). The expiratory related area receives information from an hypothetical region within the brainstem denoted as "initating area" [IA, blue circle, Fig. 2(A)]. This nucleus simultaneously sends information to both ER_e and the thalamus, represented in this model Uva [yellow circle, Fig. 2(A)]. From there, the information reaches the forebrain where HVC (green circle) is connected to RA. This latter nucleus is represented by two populations of excitatory and inhibitory neurons [RA_e and RA_i, red circle, Fig. 2(A)]. Finally RA_e projects to the respiratory circuit in the brainstem. Thus, the respiratory area processes information from IA before the contribution arrival from RA_e, resulting in a two-input-integrated cycle.

The constants for each subpopulation in the circuit are shown in Table 1.

In a similar way as the oscillating patterns, for type p2 II and type p2 III it is necessary to include a first starting pulse with the purpose of exciting the RA population.

These initial pulses fail to activate through the direct connection of IA the activity of ER [see asterisk in Figs. 2(D)– (E)]. The values used were $(F_{ia}, F_{\mathrm{HVC},e}, F_{\mathrm{HVC},i}) = (2, 10, 10)$, $(d_i, d_h) = (22ms, 36ms)$ for type II and $(F_{ia}, F_{\mathrm{HVC},e}, F_{\mathrm{HVC},i}) = (2, 14, 0)$, $(d_i, d_h) =$ $(22ms, 14ms)$ for type III.

$$X' = \frac{|Dexp - Dtheo|}{Dexp}. \qquad (3)$$

As in the previous oscillating patterns, we founda feature which allows us to identify each of the syllables of these sets obtained experimentally. Over all the set of measured p0, we observed a signif-

as characteristic parameter to minimize

Fitting of Δ

We assumed that the time of arrival and processing from IA to the telencephalon, Δ [illustrated inFig. 2(G)], was a fixed constant for each studied bird. We determined its value by selecting the experimental recorded p0 syllable whose values D_{exp} and H_{exp} were closer to the average values $\langle D_{exp}\rangle$and $\langle H_{exp}\rangle$ from all the dataset [$(\langle D_{exp}\rangle; \langle H_{exp}\rangle) = (317 \pm 51$ ms, $0, 07 \pm 0, 03)$, $N = 103$ for bird #31,
$(329 \pm 25$ ms; $0, 12 \pm 0, 07)$, $N = 110$ for bird #32

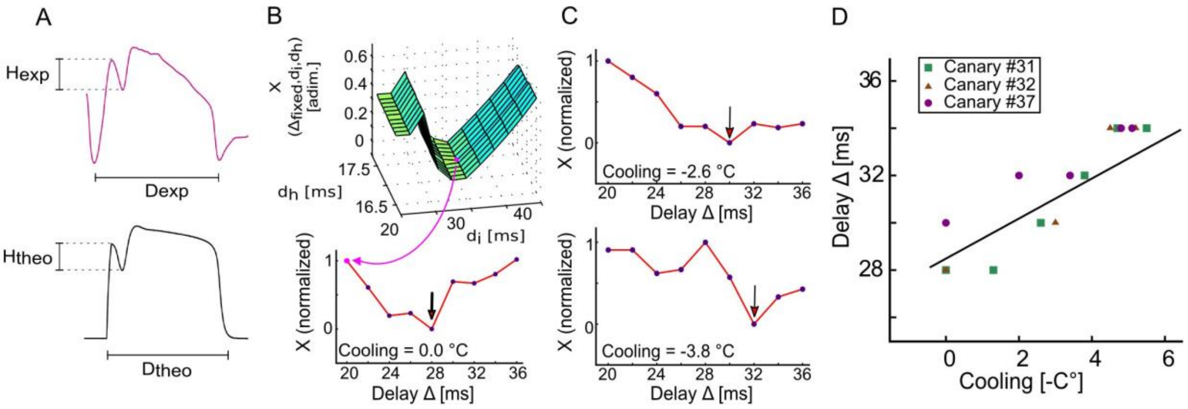

Figure 3: **Parameter space and fitting procedure for p0 syllables.** (A) Two features of p0 syllables were chosen to be fitted with the model: the total duration of gesture ($Dexp$) and the pressure difference between the first maximum and the first minimum ($Hexp$). We minimized the cost function $X = |Dexp{-}Dtheo| \;.\; |Hexp{-}Htheo|$. (B) To determine the value of Δ, the time between IA and HVC pulses, we minimized X for a representative p0 ($Dexp$ and $Hexp$ value closer to the population average) by fixing Δ and exploring the pulses duration space (top panel). Once the minimum$_{Dexp}$ was found$_{Hexp}$ (pink dot), the procedure was repeated by changing the time delay. The value of Δ that generated the minimum X (red arrow, lower panel) was taken as a constant for the rest of the simulations. (C) An increment of the Δ value was found as this procedure was repeated for all the cooling temperatures. (D) We summarize the results obtained for three different birds. As expected, time delays

are positively correlated with cooling temperatures. Slope = (1.1 ± 0.1) ms/°C, intercept = (28.2 ± 0.5) ms, R = 0.81 ±and (470 65± ms; 0, 07 0, 01), N = 32 for bird #37] and we minimized X by exploring the pulse duration space (d_i, d_h) with a fixed value of Δ [Fig. 3(B), top panel]. Each pulse length was varied in the range from 2 to 65 ms (in order to recover solutions with the morphology of p0) until the absolute minimum was found [pink dot, Fig. 3(B)]. This procedure was then repeated by changing the delay Δ in the range of 20 to 36 ms, with a step of 2 ms. This is a reasonable delay range to explore for a minimum of three synapse distance connection [22, 28,33]. Figure 3(B) —lower panel— shows the minimum value of X (normalized in the [0, 1] range) for each delay. We chose the time delay Δ as the minimum value of that curve, and we repeated the procedure for each bird studied. First, we searched its closer-to-the-mean p0 syllable and minimized X as a function of Δ for that gesture. The value obtained for birds #31 and #32 was 28 ms, while for the bird #37 it was 30 ms.

The procedures described in this section provided the parameters of the circular model that produced patterns that quantitatively match the experimental data. An example of the simulation of a complete song is observed in Fig. 4, along with the activity of each intervening nucleus. In the figure, the song starts with a set of pulsatile syllables followed by p1 patterns. The activity of IA in this part remains silent except for the beginning of each change of syllable type. Mounted on a constant DC level, the dynamics on HVC consists in a series of bursts that define the average frequency of the gestures. The p1 are followed by slower syllables: p2. As mentioned before, the beginning of each syllable starts in IA, followed by the activation in HVC, which has a different averaged DC with respect to the previous pattern. Finally, five p0 are generated by using different subpopulations of neurons in the presented architecture. This is reflected in the basal level of HVC as well as the slow dynamics in RA. In the end, the song ends with a set of pulsatile and p1 syllables. The continuous trace of the pressure output shows the capabilities of the model to link different simulated syllables together.

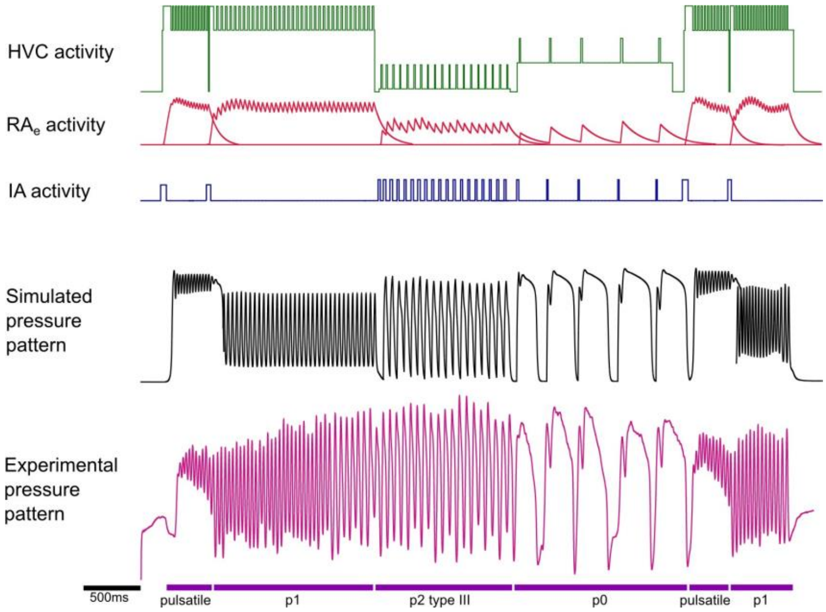

Figure 4: **A complete pressure pattern simulation based on the circular model.** In order to reproduce the respiratory pressure patterns computationally, certain features of each gesture were selected to fit the experimental data (see main text for details). For p1 and pulsatile syllables, we simulated gestures with mean oscillation frequency equal to the experimental patterns. For the p2 in this song (type III), our fitting parameter was the syllable duration. Finally, for each syllable p0, the activity in IA and HVC was varied so as to minimize X, which measure the goodness of the fit. The activity in IA is fundamentally needed to generate p0 and p2 gestures, whereas pulsatile and p1 are only produced by the activation of HVC. The baseline of the activity in HVC changes during the production of each type of syllable. The continuous trace of the pressure output shows the capabilities of the model to link different simulated syllables together. The values in Table 1 were used to generate each syllable type, while the parameters P_h, d_h, d_i were tunned for each gesture in order to reproduce its experimental feature: P_h = 41.4112 ms and P_h = 33.4010 ms (first and second p1); P_h = 29.9720 ms and P_h = 33.3576 ms (pulsatile). The values of d_i and d_h fluctuate around 20 ms and 10 ms for p2 and around 14 ms and 17 ms for p0. The time delay Δ = 28 ms was fixed for all the simulations.

Thermal control of the telencephalon affects the respiratory patterns in two ways. For mild cooling, the song slows down, which is reflected in only a stretching of their shape. This effect is compatible with the hypothesis of a top-down representation of the song motor system, as cooling would slow down the activity in HVC. However, decreasing the temperature more has critical consequences: qualitative changes in the morphology of the pressure oscillations and even breaking of the syllables into smaller pieces. Also, the structure of the complete song is broken, presenting some complete bouts,
and part of bouts or sets of syllables, sparsely distributed with extended silences between them.

Our model has the capability of translating the syllable morphological effects into changes in the parameters, since the cooling produces a slowing down of the internal dynamics of HVC, and a slowing down in the synapses from the brainstem to the telencephalic structures. Operationally, this is translated into the model by changes in the duration d_h of the driving pulses at HVC, its periodicity P_h and the delay Δ between the pulses in IA and HVC. These effects will be especially noticeable for those patterns where the two timescales interact, such as in p0. To study how these parameters

Fitting the cooling effects

Table 2: **Linear fit results.** For each experimental syllable, a set of parameters were found to recreate its feature. We adjusted the average values of these parameters with linear regressions, for the four types of syllables. For p1 and pulsatile solutions the fit was made on the variation of the period of the activity in HVC along the temperature change. For p2 and p0, we adjusted the pulse duration of HVC and IA as a function of the time delay.

Panel	Reference	Slope	Intercept	R^2
	Canary #31	$(8.53 \pm 1.79).10^{-4}$ ms/°C	$(3.17 \pm 0.09).10^{-2}$ ms	0.70
A	Canary #32	$(1.69 \pm 0.88).10^{-4}$ ms/°C	$(1.49 \pm 0.38).10^{-2}$ ms	0.25
	Canary #37	$(6.64 \pm 0.75).10^{-4}$ ms/°C	$(1.54 \pm 0.30).10^{-2}$ ms	0.92
	Canary #31	$(3.50 \pm 0.86).10^{-4}$ ms/°C	$(1.93 \pm 0.04).10^{-2}$ ms	0.61

B	Canary #32	$(6.25 \pm 0.89).10^{-4}$ ms/°C	$(2.79 \pm 0.04).10^{-2}$ ms	0.89
	Canary #37	$(6.53 \pm 1.21).10^{-4}$ ms/°C	$(2.14 \pm 0.05).10^{-2}$ ms	0.82
	Type I	0.20 ± 0.03	(4.99 ± 0.89) ms	0.93
C	Type II	0.06 ± 0.11	(22.58 ± 3.56) ms	0.31
	Type III	0.57 ± 0.12	(−3.74 ± 3.89) ms	0.92
	Type I	0.29 ± 0.23	(23.18 ± 7.10) ms	0.38
D	Type II	−0.16 ± 0.14	(23.09 ± 4.46) ms	0.13
	Type III	−0.07 ± 0.14	(25.18 ± 4.46) ms	0.36
	Canary #31	1.12 ± 0.25	(−9.44 ± 7.85) ms	0.82
E	Canary #32	0.79 ± 0.16	(−6.68 ± 4.92) ms	0.89
	Canary #37	1.00 ± 0.03	(−8.41 ± 0.95) ms	0.97
	Canary #31	0.08 ± 0.25	(39.72 ± 7.87) ms	0.05
F	Canary #32	0.08 ± 0.14	(40.89 ± 4.23) ms	0.25
	Canary #37	0.21 ± 0.46	(28.83 ± 14.88) ms	0.17

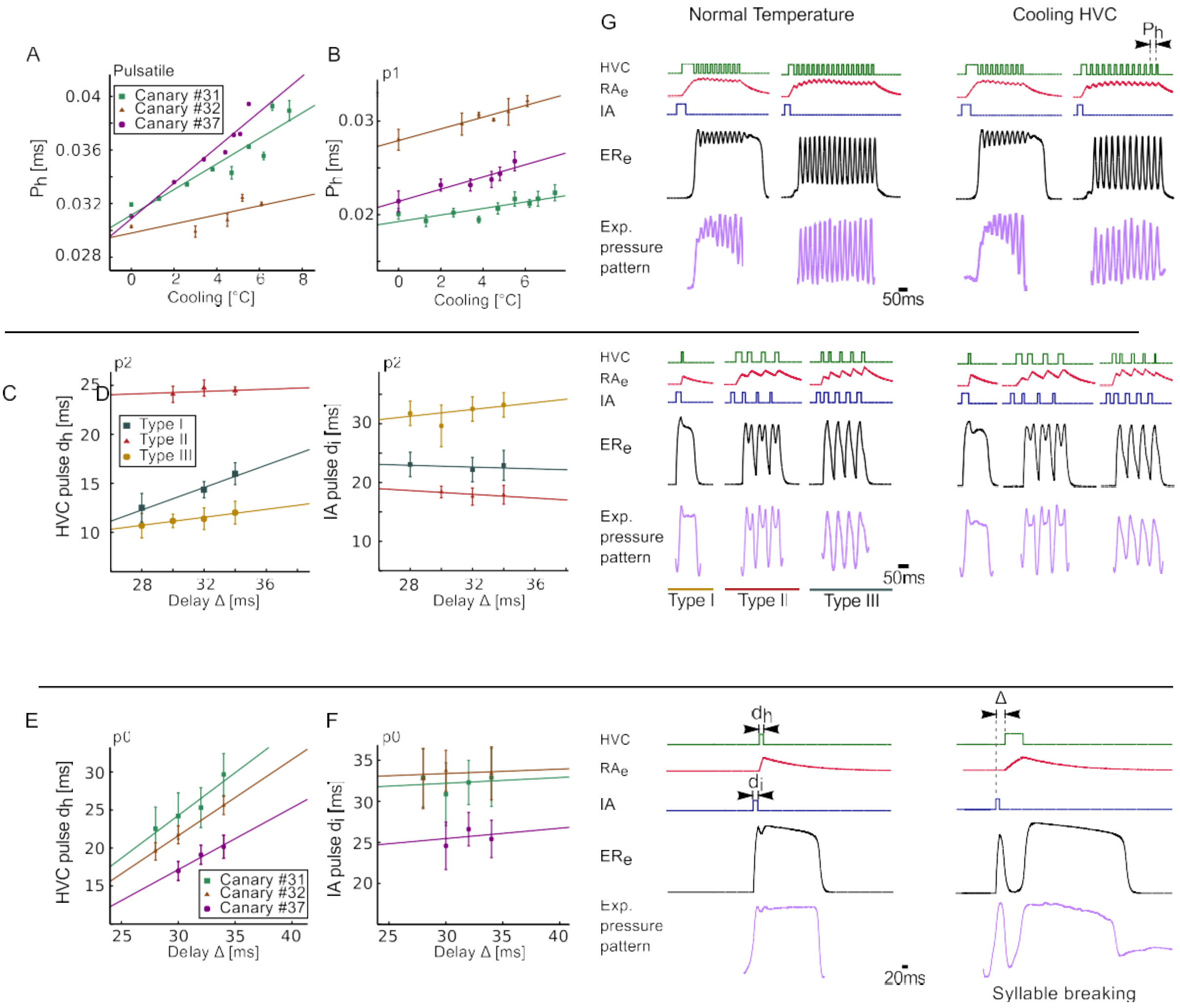

Figure 5: **Motor gesture patterns under HVC cooling.** For each syllable in the four classification groups, we set the activity in IA and HVC to recreate the selected features of the measured pressure pattern at all temperatures. For pulsatile and p1 (A)–(B), the feature varied was the forcing period P_h in HVC. For p0 and p2, it was the width of the pulses of HVC and AI, with a fixed characteristic delay at different temperatures (C)–(F). All the values are an average over all the dataset. Panel (G) shows the cooling effect for all syllables, in particular the mechanism of stretching and delay that allowed to recreate the breaking effect of a p0 syllable. Fitting values can be found in Table 2. Each gesture was generated by using the constants in Table 1 and choosing the parameters Δ, P_h, d_h, d_i that best fit the X value. For normal temperature: $P_h = 29.684$ ms (pulsatile); $P_h = 36.2818$ ms (p1); $(d_i, d_h, \Delta) = (20, 17.4, 28)$ ms for p0, (28, 9.6, 28) ms (p2 type I) and values around $d_i = 12$ ms, $d_h = 24$ ms with $\Delta = 30$ ms (p2 type II) and $d_i = 24$ ms, $d_h = 13$ ms with $\Delta = 28$ ms (p2 type III). Cooling

HVC: P_h = 33.631 ms (pulsatile); P_h = 43, 2736 ms (p1); (d_i, d_h, Δ) = (14, 67.4, 34) ms for p0, (34, 12, 34) ms (p2 type I) and values around d_i = 12 ms, d_h = 27 ms with Δ = 32 ms (p2 type II) and d_i = 24 ms, d_h = 14 ms using Δ = 32 ms (p2 type III the remarkable effects of cooling are displayed in Fig. 5(G), showing the activity in each nuclei of the model and the experimental syllable. Figure 5(G) —bottom panel— shows two syllables obtained in the simulations with the dynamics of each intervening nucleus at extreme cooling. Simulations show that only increasing the time delay the gesture fails in rising after the pulse from IA. On the other hand, stretching the activity in HVC, but leaving the delay fixed, leads to the generation of longer patterns without changes in the pressure gap.

Discussion

Our starting point was a mathematical representation proposed by Alonso *et al.* [15] that qualitatively describes the mechanisms that generate the different pressure patterns observed during the song of canaries. This vision opposes to a scenario where periodic activity in HVC is enough to generate the vast syllabic repertoire. Moving a step forward in the circular model, we quantitatively fit gesture patterns by varying the interpretable parameters that account for the activity in IA and HVC. Each syllable was classified and we extracted a characteristic feature that we aimed to reproduce numerically. By using experimental data of respiratory singing activity while cooling HVC, we were able to study how the circuit dynamics change in terms of temporal coding.

Our analysis starts with two types of syllables presenting a periodic behavior: p1 and pulsatile. To simulate these patterns, we proposed a periodic activity in HVC with period P_h. Then, for each experimental syllable, we adjusted P_h so that the average frequency of the whole gesture matched the average frequency of the experimental syllable. As HVC was cooled, experimental motor gestures were stretched. Simulations showed that increasing the forcing period parameter was enough to reproduce the syllables since no qualitatively changes in the morphology of the simulated patterns were observed when varying the pulse length.

On the one hand, since the generation of these types of syllables is mainly ruled by the flow of information downstream from HVC to the brainstem, both circular and clock models are compatible. Moreover, both frameworks agree that the decrease of the frequency of HVC is an expected effect as the nucleus is cooled, resulting in a stretching of the pressure patterns. On the other hand, respiratory motor gestures with richer structure, such as p0 and p2, provided us the key to decide between the two models, since the cooling affects not only the duration of the syllable but also its internal structure. For example, at low temperatures, p0 patterns show an increase of the pressure gap after the first maximum of pressure. To explain these phenomena, we proposed that at least two timescales must be involved in the generation of the gesture. This hypothesis was tested by modeling the activity in IA and HVC with simple pulses of duration d_i and d_h respectively, separated by a fixed time Δ. If a unique timescale is involved in the generation of the motor gestures, these three parameters should change as a result of thermal manipulation of the circuit. We first associated the time delay Δ to each temperature variation by studying the morphology changes of the p0 syllables. We showed that this parameter must increase as a result of cooling HVC [Fig. 3(D)]. Letting the remaining two parameters vary independently, we searched for the ones that generated a pressure pattern having the feature of each of our experimental recorded gesture. On the one hand, Figs. 5(D)–(F) show that the dynamics of IA remains practically unalterable during cooling, in the generation of p2 and p0 syllables. On the other hand, the duration of the pulses in HVC are affected in several ways while cooling. For p2, cooling has minimal effect in type III gestures and a slight increase of duration in type II syllables [Fig. 3(C)]. However thermal manipulation in this area exerts a stronger effect in type I and p0 syllables. This result may shed light on the need of more than one timescale, as one timescale is slowed by the cooling effect, the other remains immutable and therefore only a fraction of the entire syllable is modified. Note that although for all syllables cooling HVC results in a slowdown of its activity, lower frequency syllables reflect the stretching of pulses in HVC.

Under the hypothesis of the circular model, the breaking of the p0 syllables can be easily interpreted. The first peak of pressure is the result of the arrival of the activity from IA. Pressure then rises again as the signal of RA reaches the respiratory related area. As the temperature decreases, the separation between the two signals increases, causing the pressure to drop after reaching its maximum value. A larger signal from RA is needed in order to rise the pressure back. This is accomplished by stretching the pulses within HVC. Remarkably, both effects —increasing the time delay between pulses and stretching the length of HVC pulses— are needed to recreate the breaking, and are compatible with the HVC cooling effects.

Conclusions

In this work, we tested the hypothesis that at least two separate timescales are responsible for the generation of the respiratory motor gestures during birdsong production. We studied quantitatively the deformations of the air sac pressure patterns of syllables under temperature changes in terms of interpretable parameters of a circular model, that account for the activity in brain areas related to motor gesture generation.

We proposed that syllables with simple internal structure (p1 and pulsatile) emerge from periodic activity in the telencephalic nucleus HVC. Decreasing the temperature in this nucleus produces a slowdown that increased the period of the pressure patterns. This is translated in the model as an increase of the time between pulses within HVC.

As HVC is cooled, gestures with richer internal structure (p2 and p0) suffer from qualitative changes in their morphology, leaving other features immutable. These phenomena may suggest the interaction of two different time scales. The second responsible timescale is proposed to emerge from a region within the brainstem (IA), which also projects to HVC. To test this hypothesis, we focused our study in the variation of the dynamics of IA and HVC needed to recreate gestures displaying the same morphology changes as observed experimentally. These dynamics were represented as sparse bursts of information of independent duration, beginning from IA and processed in HVC a time Δ later. Our results showed that the time delay between these pulses must increase in order to quantitatively fit the pressure patterns from cooled HVC. We also showed a positive correlation between the duration of the pulses from HVC and the time delay Δ, while the size of the pulses in IA remains unaltered. Therefore, reducing the temperature in HVC is represented in the model by two phenomena: a slowdown of the activity in HVC and an increase of the delay between pulses from IA. This is compatible with the hypothesis that cooling the HVC area results in delaying synaptic inputs into HVC and also delaying intrinsic synapses within HVC. Both effects are needed in order to generate quantitatively the cooled gestures. Moreover, the fact that the activity in IA results practically constant across all temperatures leads us to picture the system as a jazz band where the rhythms emerge from the interaction of many musicians instead of an orchestra with its director. This is in agreement with recent physiological experiments measuring the processing time between HVC and Uva while thermally manipulating each nucleus [22], and experimental modeling of the synaptic delays in HVC neurons [24], which supports the hypothesis of a distributed timescale among the brain song net- work.

Reference

H P Zeigler, P Marler, *Neuroscience of birdsong*, Cambridge University Press, Cambridge(2008).

J M Wild, *Neural pathways for the control of birdsong production*, Dev. Neurobiol. **33**, 653 (1997).

F Nottebohm, *The neural basis of birdsong*,

F Goller, R A Suthers, *Role of syringeal muscles in gating airflow and sound production in singing brown thrashers*, J. Neurophysiol. **75**, 867 (1996).

G B Mindlin, T J Gardner, F Goller, R Suthers, *Experimental support for a model of birdsong production*, Phys. Rev. E **68**, 041908(2003).

M F Schmidt, F Goller, *Breathtaking songs: Coordinating the neural circuits for breathing and singing*, Physiology **31**, 442 (2016).

G Angle, H Coskun, *A complete syllable dictionary for Serinus canarius*, Ecol. Inf. **20**, 67 (2014).

J A Alliende, J M Mndez, F Goller, G B Mindlin, *Hormonal acceleration of song development illuminates motor control mechanism in canaries*, Dev. Neurobiol. **70**, 943 (2010).

R H Hahnloser, A A Kozhevnikov, M S Fee, *An ultra-sparse code underlies the generation of neural sequences in a songbird*, Nature **419**, 6902 (2002).

M S Fee, A A Kozhevnikov, R H Hahnloser, *Neural mechanisms of vocal sequence gener-*

PLoS Biol. **3**, e164 (2005).

R C Ashmore, J M Wild, M F Schmidt, *Brain-stem and forebrain contributions to the gener- ation of learned motor behaviors for song*, J. Neurosci. **25**, 37 (2005).

R H Hahnloser, A Kotowicz, *Auditory representations and memory in birdsong learning*, Curr. Opin. Neurobiol. **20**, 332 (2010).

F Goller, R A Suthers, *Role of syringeal muscles in controlling the phonology of bird song*, J. Neurophysiol. **76**, 287 (1996).

ation in the songbird, Ann. NY. Acad. Sci. **1016**, 153 (2004).

M A Long, M S Fee, *Using temperature to analyse temporal dynamics in the songbird motor pathway*, Nature **456**, 189 (2008).

R G Alonso, M A Trevisan, A Amador, F Goller, G B Mindlin, *A circular model for songmotor control in Serinus canaria*. Front. Com-put. Neurosci. **9**, 1 (2015).

A Amador, S Boari, G B Mindlin, *From perception to action in songbird production: Dynamics of a whole loop*, Curr. Opin. Syst. Biol.**3**, 30 (2017).

R Bertram, A Daou, R L Hyson, F Johnson, W Wu, *Two neural streams, one voice: Pathways for theme and variation in the songbird brain*, Neuroscience **277**, 806 (2014).

M F Schmidt, J M Wild, *The respiratory-vocal system of songbirds: Anatomy, physiology, and neural control*, Prog. Brain Res. **212**, 297 (2014).

M A Goldin, L M Alonso, J A Alliende, F Goller, G B Mindlin, *Temperature induced syl- lable breaking unveils nonlinearly interacting timescales in birdsong motor* *pathway*, PLoS One **8**, e67814 (2013).

M A Goldin, G B Mindlin, *Evidence and control of bifurcations in a respiratory system*, Chaos **23**, 043138 (2013).

A S Andalman, J N Foerster, M S Fee, *Control of vocal and respiratory patterns in birdsong: Dissection of forebrain and brainstem mecha- nisms using temperature*, PLoS One **6**, e25461 (2011).

K Hamaguchi, M Tanaka, R Mooney, *A distributed recurrent network contributes to temporally precise vocalizations*, Neuron **91**, 1 (2016).

Y S Zhang, J D Wittenbach, D Z Jin, A A Kozhevnikov, *Temperature manipulation insongbird brain implicates the premotor nucleusHVC in birdsong syntax*, J. Neurosci. **37**, 2600(2017).

R C Ashmore, J A Renk, M F Schmidt, *Bottom-up activation of the vocal motor forebrain by the respiratory brainstem*, J. Neurosci. **28**, 2613 (2008).

R A Suthers, S A Zollinger, *Producing song: The vocal apparatus*, Ann. NY. Acad. Sci. **1016**, 109 (2004).

F C Hoppensteadt, E M Izhikevich, *Weakly connected neural networks*, Springer, New York (1997).

J S McCasland, M Konishi,*Interaction between auditory and motor activities in an avian song control nucleus,* P. Natl. Acad. Sci. USA **78**, 7815 (1981).

A Amador, Y S Perl, G B Mindlin, D Margoliash, *Elemental gesture dynamics are encoded by song premotor cortical neurons*, Nature **495**, 59 (2013).

R Mooney, J F Prather, *The HVC microcircuit: The synaptic basis for interactions between song motor and vocal plasticity pathways*, J. Neurosci. **25**, 1952 (2005).

M A Goldin, G B Mindlin, *Temperature manipulation of neuronal dynamics in a forebrain motor control nucleus*, PLoS Comput. Biol. **13**, e1005699 (2017).

D Galvis, W Wu, R L Hyson, F Johnson, R Bertram, *A distributed neural network model for the distinct roles of medial and lateral HVC in zebra finch song production*, J. Neurophys-iol. **118**, 677 (2017).

J Kornfeld, S E Benezra, R T Narayanan, F Svara, R Egger, M Oberlaender, W Denk, M A Long, *EM connectomics reveals axonal target variation in a sequence-generating network*, eLife **6**, e24364 (2017).

M F Schmidt, R C Ashmore, E T Vu, *Bilateral control and interhemispheric coordination in the avian song motor system*, Ann. NY. Acad. Sci. **1016**, 171 (2004).